Hybrid FEM-MFS Modeling of Low-Height Sonic Crystal Noise Barriers with Embedded Resonators

Luís Godinho[1], Nicolas Herrera-León[1], Paulo Amado-Mendes[1]

[1]*ISISE, ARISE, Department of Civil Engineering, University of Coimbra, Portugal*

Abstract

This work presents a frequency-domain numerical model based on the coupling of the Finite Element Method (FEM) and the Method of Fundamental Solutions (MFS) for the analysis and design of low-height sonic crystal noise barriers with embedded resonators. The application focus is the mitigation of railway-induced noise from trains and trams, in configurations where the barriers are placed in close proximity to the track. Detailed modeling of the barrier geometry, resonant inclusions, and near-field acoustic effects is achieved using the FEM, which also includes a limited region of the surrounding air to accurately describe the local wave–structure interaction. The MFS is subsequently employed to represent the unbounded acoustic domain, allowing the correct treatment of sound radiation and propagation in an infinite half-space without truncation or artificial boundary conditions. The proposed coupled FEM–MFS strategy enables an efficient and accurate numerical assessment of metamaterial-based noise barriers in realistic deployment scenarios. Numerical examples are presented to demonstrate the influence of resonator design and barrier placement on acoustic attenuation performance, highlighting the capabilities and potential of the method for railway noise control applications.

Keywords: *sonic crystal, FEM-MFS coupling, embedded resonators, railway noise*

1. Introduction

Railway and light-rail transportation are essential to modern urban mobility, yet the noise from trains and trams remains a major source of environmental disturbance for nearby populations [1]. Noise barriers (NBs) are the most common mitigation strategy, typically built as continuous solid walls of concrete, wood or metal [2]. However, to be effective they generally need to be tall and continuous, raising construction costs, creating visual impact, and often conflicting with the reduced clearance and near-track placement required in railway environments.

Acoustic metamaterials, and in particular sonic crystals (SCs), have emerged as a promising alternative. SCs consist of a spatially periodic arrangement of scatterers in a fluid medium, whose periodicity produces frequency bands – the so-called band gaps – within which sound propagation is strongly attenuated due to the Bragg effect [3]. This has motivated extensive research on SCs as noise barriers, with studies showing that periodic arrangements of rigid or coated cylinders achieve significant attenuation, offering a lighter, more transparent alternative to solid barriers [4,5].

Since the attenuation of a rigid SC is largely confined to the Bragg band gap, several strategies have been proposed to broaden its performance. Absorptive coatings, such as porous layers, improve attenuation both within and beyond the band gap [6], including in low-height configurations designed for placement near the railway track [7]. Embedded Helmholtz resonators introduce additional, tunable attenuation peaks at target frequencies, such as train braking [8], and further increase insertion loss when combined with absorptive layers [9,10]. Since trains and trams radiate significant noise near the track at low-to-mid frequencies [11], combining a SC with a porous coating and embedded resonators suits low-height barrier design well. Here, the coating is characterized using the Horoshenkov–Swift model [12], with parameters from porous concrete samples in [13].

Numerically, however, such barriers combine a locally complex geometry – resonant cavities and absorptive coatings – with propagation into a semi-infinite domain. The Finite Element Method (FEM) captures local detail well but needs added techniques, such as Perfectly Matched Layers (PML), to represent the unbounded exterior, at significant cost. Meshless approaches such as the Method of Fundamental Solutions (MFS), using periodic Green's functions

Corresponding author: *lgodinho@dec.uc.pt.*

developed for sonic crystal structures [14], represent semi-infinite and periodic domains efficiently without truncation, but are less suited to complex local geometries. To combine both strengths, this paper proposes a hybrid FEM-MFS coupling, using a limited FEM region for the barrier's scatterers, coating and resonators, and the MFS for the surrounding unbounded domain.

The remainder of this paper is organized as follows. First, the FEM-MFS coupling formulation is presented, including the periodic Green's functions used for the semi-infinite domain above a rigid ground. The approach is then verified against a reference full FEM model with a PML, for a three-row sonic crystal barrier with a porous coating. Finally, an application example with embedded Helmholtz resonators illustrates the model's potential for designing low-height sonic crystal barriers with enhanced, broadband performance for railway and tram noise mitigation.

2. Mathematical formulation

The formulation proposed here couples a 3D Finite Element (FEM) limited region with an external, unbounded, region modelled using the Method of Fundamental Solutions (MFS).

Since both FEM and MFS are well known and can easily be found in the literature, only a very brief overview is given here regarding each of the methods.

For the FEM, the standard formulation is used, based on the assemblage of stiffness (K) and mass (M) matrices of the system, leading to the conventional equation for an harmonic response at angular frequency $\omega = 2\pi f$:

$$[K - \omega^2 M]P = F \tag{1}$$

Here, P is the unknown pressure vector, and K and M are assembled considering the domain to be discretized using quadratic tetrahedra, with 10 nodes per element, and F includes the effect of external forces and boundary conditions.

As for the MFS, its meshless formulation is based on the prior knowledge of the Green's functions for the specific problem to be solved. For the present case, since a periodic problem is considered, the following Green's functions are used (derived by Godinho et al [14]), also considering the presence of an infinite rigid ground at z=0.0:

$$G(\boldsymbol{x}_l^v, \boldsymbol{x}) = -\frac{i}{4a}\left(\sum_{n=-\infty}^{+\infty}\left(H_0^{(2)}(k\,r\,) + H_0^{(2)}(k\,'r\,'\,')\right)e^{-i\times\frac{2\pi}{a}\times n\times(y-y_0)}\right) \tag{2}$$

In which $\boldsymbol{a}$ is the periodicity along the axis y, and $\boldsymbol{x}_l^v$ is the position of the source and $\boldsymbol{x}$ is the receiver position. Additionally,

$$k\,' = \sqrt{\left(\frac{\omega}{c}\right)^2 - k_y^2}\ (\mathrm{imag}(k\,') < 0) \tag{3}$$

$$r\,' = \sqrt{(x - x_0)^2 + (z - z_0)^2} \tag{4}$$

$$r\,'\,' = \sqrt{(x - x_0)^2 + (z + z_0)^2} \tag{5}$$

The pressure field in the MFS is simulated as a linear combination of Green's functions (equation 2), based on a number of virtual sources positioned outside the propagation domain, and can thus be can be written as

$$p(\boldsymbol{x}) = \sum_{l=1}^{NVS} A_l G(\boldsymbol{x}_l^v, \boldsymbol{x}) + P_{inc}(\boldsymbol{x}), \tag{6}$$

where A_l are unknown coefficients that can be determined after establishing a system of equations in which the necessary boundary conditions are imposed, and $P_{inc}(\boldsymbol{x})$ represents the effect of possible sources in the domain (incident field).

To build the proposed coupled MFS-FEM strategy, a direct and explicit coupling is adopted here. However, to render the method flexible, non-matching positions between the FEM nodes and the collocation points of the MFS are allowed. The coupling matrix can be represented, compactly, as:

$$\begin{bmatrix} K - \omega^2 M & A \\ \varphi & B \end{bmatrix}\begin{bmatrix} P_{FEM} \\ X_{MFS} \end{bmatrix} = \begin{bmatrix} F_{FEM} \\ P_{inc} \end{bmatrix} \tag{7}$$

The coupling is performed in a contact surface between the two subdomains, ensuring continuity of normal particle velocities and pressures between both. Here, A and B represent MFS generated matrices respectively related to the integrated velocity (A) over the finite element faces in the contact surface, and to the pressure continuity at the MFS collocation points; consequently, $\boldsymbol{\varphi}$ is nothing more than an interpolation matrix for the pressure between FEM nodes and MFS collocation points. F_{FEM} corresponds to the effect of a possible source located in the MFS part of the domain over the interface between FEM and MFS in terms of particle velocity, and P_{inc} represents the effect of the same source in terms of pressure.

3. Verification of the proposed approach

To verify the proposed formulation, a simple case of a periodic structure is considered, consisting of a sonic crystal with three rows (in the x direction), and with scatterers 1.0m tall (in the z direction). The scatterers are spaced 0.17m between them along the x and y axes, thus leading to an infinitely periodic structure along the y direction. The internal part of the scatterers is rigid, but a porous layer with a thickness of 0.02m is

considered covering their surface. The external diameter of the scatterers thus becomes 0.12m.
The porous layer is simulated by using the Horoshenkov-Swift model [12], considering a porosity of 39%, an airflow resistivity of 5428 Pa.s/m2, a tortuosity of 2.27, and a standard deviation of the pore size of 0.25. The host fluid medium is assumed to be air, with a density of 1.21 kg/m^3 and allowing sound to travel with a velocity of 343 m/s.
The system is excited by a source at located at x=-1.0m, and the response is calculated for a frequency of 500Hz using both a standard FEM implementation, making use of a PML to simulate the semi-infinite character of the propagation domain, and using the proposed MFS-FEM coupling, in which the infinite character is automatically accounted for by the MFS part.

Figure 1 illustrates the FEM model, considering a semi-circular cylindrical domain with a radius of 2.5m, in which the outer 0.5m correspond to the PML. A total of 504651 tetrahedra and 751406 nodes are used in this discretization. The dark blue color represents the host fluid (air) and the light blue, green and yellow correspond to the porous layers surrounding the first, second and third scatterers.

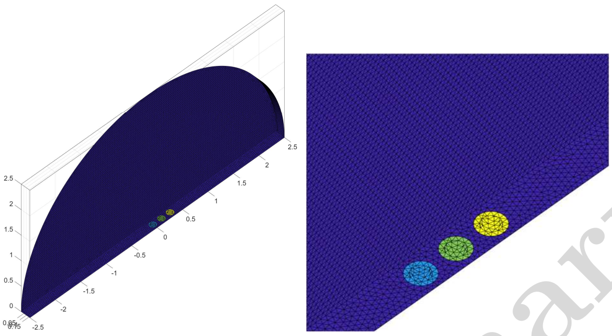

a) b)

Figure 1. Mesh used for the FEM reference model: a) global view; b) detail of the bottom of the mesh including the scatterers.

As for the FEM-MFS model, a schematic of the discretization is presented in Figure 2. Here, Figure 2a represents the MFS part, including both the collocation points (blue) and virtual sources (red), and Figure 2b represents the FEM discretization, with just 43454 elements and 68745 nodes. The reduction in the total number of elements and nodes is very clear, considering that the MFS only makes use of 784 collocation points and sources.
Figure 3 illustrates the pressure level computed by both models for the given frequency of 500Hz, clearly revealing a very good match between them. For the case of the FEM, the effect of the included PML is visible, effectively attenuating the sound pressure level along the circular boundary, and thus minimizing spurious reflections. In the case of the MFS-FEM, no such artificial boundaries are required, and the presented SPL shows no traces of any such reflections.

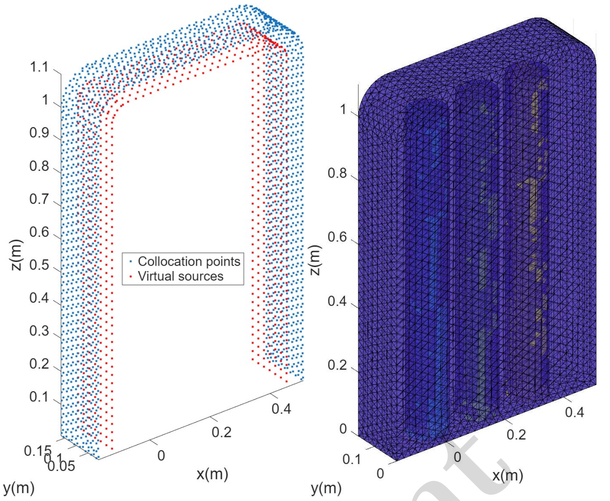

Figure 2. MFS points and mesh used for the FEM in the coupled model: a) MFS collocation points and virtual sources; b) FEM part of the coupled model.

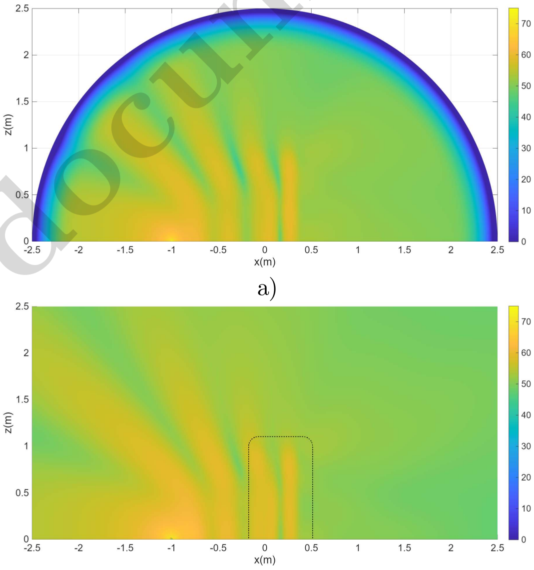

a)

b)

Figure 3. Results obtained by the two models for 500Hz in terms of sound pressure level: a) Full FEM model; b) MFS-FEM model.

For both models, the effect of the sonic crystal is visible, with part of the energy being reflected back to the source region, and a clear reduction of the sound pressure level registered behind the sonic crystal barrier.

4. Application example

The coupled approach proposed in this paper has been applied to determine the insertion loss throughout the frequency domain for a more complex sonic crystal noise barrier. For this, a sonic crystal similar to the one described in the previous section has been used, but additionally considering the incorporation of embedded resonators in the scatterers. In this case, 12 resonators (consisting of 3 sets of 4 resonators with resonance frequencies of 360Hz, 440Hz, 560Hz and 615Hz) have been included. The MFS-FEM coupled approach was used considering the FEM region as depicted in Figure 4a. Figure 4b shows a detail of the inclusion of the resonant elements within the scatterers of the sonic crystal

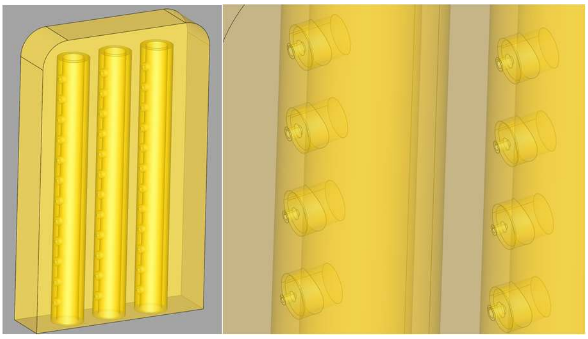

Figure 4. Application example model: a) overview of the part of the domain to be discretized with FEM; b) detail of the resonant elements embedded within the sonic crystal scatterers.

For this geometry, the insertion loss was computed as the difference between sound pressure levels in the scenarios without and with the barrier, over a dense grid of 2440 receivers located behind the barrier between x=1.0m and x=2.5m, and between y=0.025m and y=1.0m.

The corresponding result is presented in Figure 5. In this figure, several interesting aspects can be seen. First, the presence of the high attenuation related to the Bragg effect around 1000Hz is clear, reaching an attenuation of around 15dB. Additionally, the effect of the porous layers coating the scatterers is also evident, particularly in the valley around 1500Hz, in which a visible attenuation is still noticeable. For a case without such coating, near zero attenuation would be registered. Finally, at the resonance frequencies of the resonators, sharp peaks are registered, with significant attenuation, clearly showing that these elements are correctly taken into account.

5. Conclusions

The present paper presented a coupled approach between the Method of Fundamental Solutions and the Finite Element Method to solve complex periodic acoustic problems in the frequency domain. The model takes advantage from the capacity of the MFS to account for open domains, and of the FEM to include detailed geometries. The method was verified against a standard FEM model showing a very good match between results for the two methods.

An application example for a complex geometry was presented, including a low-height sonic crystal noise barrier with embedded resonators and a porous coating layer. The results show the expected behavior, with the main dynamic phenomena being evident.

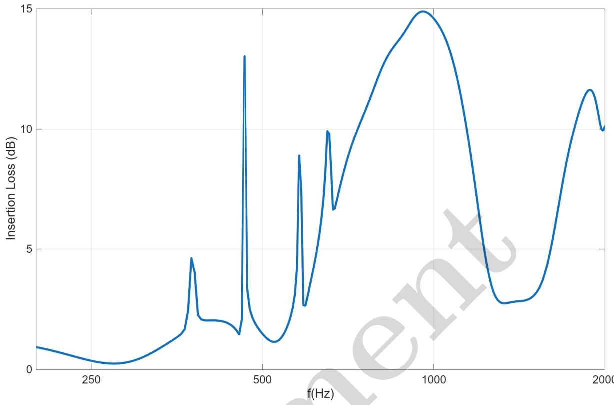

Figure 5. Insertion loss calculated for the sonic crystal noise barrier with embedded resonators.

6. Acknowledgments

This work was funded by national funds through FCT – Fundação para a Ciência e a Tecnologia, I.P., under the project NASC4Railways, with reference 2024.17219.PEX - https://doi.org/10.54499/2024.17219.PEX.
This work was also supported by FCT/MCTES under the R&D Unit Institute for Sustainability and Innovation in Structural Engineering (ISISE), under the references UID/4029/2025 (https://doi.org/10.54499/UID/04029/2025) and UID/PRR/04029/2025 (https://doi.org/10.54499/UID/PRR/04029/2025), and under the Associate Laboratory Advanced Production and Intelligent Systems ARISE under reference LA/P/0112/2020 (https://doi.org/10.54499/LA/P/0112/2020).

References

[1] E. Panulinova and S. Harabinova: "Noise annoyance from tram traffic in the urban environment," Civil and Environmental Engineering, vol. 18, pp. 688–694, 2022.

[2] E. Murphy and E. A. King: "Noise mitigation approaches," in Environmental Noise Pollution, ch. 7, pp. 203–245, Elsevier, Boston, 2014.

[3] M. S. Kushwaha, P. Halevi, L. Dobrzynski, and B. Djafari-Rouhani: "Acoustic band structure of periodic elastic composites," Phys. Rev. Lett., vol. 71, pp. 2022–2025, 1993.

[4] L. Fredianelli, L. G. Del Pizzo, and G. Licitra: "Recent developments in sonic crystals as

barriers for road traffic noise mitigation," Environments, vol. 6, no. 2, 2019.

[5] J. Sánchez-Dehesa, V. M. Garcia-Chocano, D. Torrent, F. Cervera, S. Cabrera, and F. Simon: "Noise control by sonic crystal barriers made of recycled materials," J. Acoust. Soc. Am., vol. 129, no. 3, pp. 1173–1183, 2011.

[6] O. Umnova, K. Attenborough, and C. M. Linton: "Effects of porous covering on sound attenuation by periodic arrays of cylinders," J. Acoust. Soc. Am., vol. 119, no. 1, pp. 278–284, 2006.

[7] J. Lázaro, M. Pereira, P. A. Costa, and L. Godinho: "Performance of low-height railway noise barriers with porous materials," Applied Sciences, vol. 12, no. 6, 2022.

[8] D. Ramírez-Solana, J. Galiana-Nieves, R. Picó, J. Redondo, V. Sangiorgio, A. V. Graziano, and N. Parisi: "Sonic crystal noise barrier with resonant cavities for train brake noise mitigation," Applied Sciences, vol. 14, no. 7, 2024.

[9] E. F. Vergara, G. N. Almeida, L. R. Barbosa, A. Lenzi, and A. Sousa: "Broadband and low-frequency sound absorption of modified Helmholtz resonator combined with porous layer addition," J. Appl. Phys., vol. 132, no. 13, 135114, 2022.

[10] J. Redondo, D. Ramírez-Solana, and R. Picó: "Increasing the insertion loss of sonic crystal noise barriers with Helmholtz resonators," Applied Sciences, vol. 13, no. 6, 2023.

[11] J. Lázaro, P. A. Costa, and L. Godinho: "Experimental light rail traffic noise assessment in a metropolitan area," Applied Sciences, vol. 14, no. 3, 2024.

[12] K. V. Horoshenkov and M. J. Swift: "The acoustic properties of granular materials with pore size distribution close to log-normal," J. Acoust. Soc. Am., vol. 110, no. 5, pp. 2371–2378, 2001.

[13] M. Pereira, J. Carbajo, L. Godinho, P. Amado-Mendes, D. Mateus, and J. Ramis: "Acoustic behavior of porous concrete. Characterization by experimental and inversion methods," Materiales de Construcción, vol. 69, no. 336, 202, 2019.

[14] L. Godinho, J. Redondo, P. Amado-Mendes: "The method of fundamental solutions for the analysis of infinite 3D sonic crystals". Engineering Analysis with Boundary Elements, 98, 172-183, 2019.